# Photogrammetric Deflection Measurements for the Tiltrotor Test Rig (TTR) Multi-Component Rotor Balance Calibration

**Eduardo Solis**
Industrial Design Engineer
Monterey Technologies, Inc
Moffett Field, CA, U.S

**Larry Meyn**
Mechanical Engineer
NASA Ames Research Center
Moffett Field, CA U.S

## ABSTRACT

Calibrating the internal, multi-component balance mounted in the Tiltrotor Test Rig (TTR) required photogrammetric measurements to determine the location and orientation of forces applied to the balance. The TTR, with the balance and calibration hardware attached, was mounted in a custom calibration stand. Calibration loads were applied using eleven hydraulic actuators, operating in tension only, that were attached to the forward frame of the calibration stand and the TTR calibration hardware via linkages with in-line load cells. Before the linkages were installed, photogrammetry was used to determine the location of the linkage attachment points on the forward frame and on the TTR calibration hardware. Photogrammetric measurements were used to determine the displacement of the linkage attachment points on the TTR due to deflection of the hardware under applied loads. These measurements represent the first photogrammetric deflection measurements to be made to support 6-component rotor balance calibration. This paper describes the design of the TTR and the calibration hardware, and presents the development, set-up and use of the photogrammetry system, along with some selected measurement results.

## NOTATION

| | | |
|---|---|---|
| AF | = | axial force, positive along the x-axis |
| NF | = | normal force, positive along the z-axis |
| PM | = | pitch moment, positive about the z-axis |
| RM | = | roll moment, positive about the z-axis |
| SF | = | side force, positive along the y-axis |
| TQ | = | torque, positive about the x-axis |

## ABBREVIATIONS

| | |
|---|---|
| TTR | tiltrotor test rig |
| RTA | rotor test apparatus |
| LRTA | large rotor test apparatus |
| NFAC | National Full-Scale Aerodynamics Complex |
| SketchUp | 3D modeling software |
| V-STARS | video-simultaneous triangulation and resection system |
| V-STARS/S | single camera system |
| V-STARS/M | dual-camera system |
| 80/20 | modular aluminum t-slot framing hardware |
| ROI | region of interest |
| DOF | degrees of freedom |
| DEO | design of experiment |

## INTRODUCTION

The Tiltrotor Test Rig (TTR) is a national facility that will enable advanced, large-scale tiltrotor technology testing at speeds up to 300 kts. The TTR, a NASA project joint with the Army and Air Force, can test proprotors up to 26 ft in diameter in the National Full-Scale Aerodynamic Complex (NFAC).

The TTR is designed for use in the NFAC's 40- by 80- and the 80- by 120-Foot wind tunnels. The TTR is a horizontal axis rig that mounts on the test-section turntable, enabling testing at high speeds (300 knots) in axial flight or edgewise flight at low speeds (100 knots), or at any angle in between as shown in Fig. 1. The TTR is designed to accommodate a variety of rotor types: articulated, gimbaled, soft-in plane, and rigid rotors up to 26-feet in diameter. The power, speed and aerodynamic load capabilities of the TTR are necessary to provide critical data to validate state-of-the-art design and analytical tools needed to develop future advanced rotorcraft concepts. To keep pace with the progress in higher fidelity computational tools, methods for improving the accuracy of rotor performance measurements are required.

The first test entry for the TTR is a system validation test using an existing rotor (Bell 609) in the 40- by 80- test section. The TTR must go through a series of system and hardware checkouts before this initial test entry (planned in 2016). Most important, the internal multi-component rotor balance must

Presented at the AHS Technical Meeting on Aeromechanics Design for Vertical Lift, San Francisco, California, January 20-22, 2016. 

be calibrated to accurately measure the total forces and moments generated by the rotor system. To simulate the range of rotor forces and moments on the TTR, NASA designed calibration hardware to apply loads to the rotor shaft and the internal rotor balance.

To accurately calibrate the rotor balance, the actuators on the calibration stand must be aligned with the calibration body to minimize force interactions. Deflection measurements of the rotor shaft and calibration body under load are necessary to accurately determine the location and direction of applied loads, since an inch of deflection could result in off-axis forces in excess of 100 lb for the calibration range of the TTR.

Multi-component rotor balance calibrations have long been a challenge to the rotorcraft community. The challenge of both measuring hardware deflections and minimizing hardware misalignment to reduce balance calibration uncertainty is not new, but a standard approach has not been fully developed. NASA developed the Rotor Test Apparatus (RTA) in the mid 1970's and the Large Rotor Test Apparatus (LRTA) in the 1990's to test small-and large-scale rotor systems as described in Refs. 1-3. Based upon the RTA experience (Ref. 1), the LRTA included the design of a calibration stand, which enabled an LRTA-installed rotor balance calibration. Deflection measurements using a laser tracker were acquired during the LRTA balance calibration. The applied calibration loading was corrected with the deflections measurements as described in Ref. 2. The orientation and the complex design of the LRTA calibration rig limited the deflection measurements to one rotor quadrant of the loading tree.

A multi-component balance calibration was performed on the TTR in an effort to enhance NASA's capability to accurately measure rotor performance for full-scale rotor tests. To enable hardware deflection measurements in all rotor quadrants, the calibration of the installed rotor balance utilized photogrammetry techniques to identify the line of action (load path). The deflection measurements result in accurate measurements of the off-axis forces to correct the applied loading, thus, reducing the uncertainty in the calibration.

This paper describes the calibration rig, TTR rotor balance, design and installation of the alignment hardware, the deflection hardware, and the photogrammetric measurement system. The overall calibration system design was largely driven by the constraints imposed by the TTR, the calibration stand, and the calibration body. These constraints and other challenges are discussed, along with some selected measurement results.

## CALIBRATION SYSTEM DESCRIPTION

The TTR calibration stand was designed to minimize deflections during loading. The major components of the calibration system are: the FWD Frame, the AFT Frame, the calibration body (attached to the TTR), the hydraulic actuator load system, the data acquisition system, and the photogrammetry system.

The calibration stand consists of a two subassemblies, the FWD Frame and the AFT Frame. The FWD Frame provides a rigid support for the non-metric end of the hydraulic actuators. The AFT Frame provides rigid support for the calibration body and is attached to three struts using a ball-socket interface. The FWD Frame and the AFT Frame are bolted to each other at the base and interface beams provide structural support to minimize deflection when applying single-and multi-component loads to the calibration body. Figure 2 shows the TTR installed on the calibration stand.

The calibration body (metric hardware) provides the interface between the load actuators and the rotor shaft, and allows for two calibration ranges; the expected load range for the first wind tunnel test entry (BA609 rotor) and the design load range of the rotor balance. In order to apply the two calibration ranges, the metric hardware was designed to allow for three base hardware configurations. For configuration 1, normal force and torque loads are applied to the rotor shaft and all other loads are applied to the balance. In configuration 2, no loads are applied to the rotor shaft while loads are applied to the balance. In configuration 3, normal force, torque and shear loads are applied to the rotor shaft and all other loads are applied to the balance. Figure 3 depicts the three hardware configurations.

The loading system consists of the anchor hardware, the metric hardware, and the interface hardware, which provides the mechanical connection between the calibration frame and the calibration body. The anchor hardware is mounted on the FWD Frame. A total of eleven linkages with in-line load cells and hydraulic actuators, operating in tension only, were used to apply the calibration loads as shown in Fig. 4.

## ROTOR BALANCE DESCRIPTION

The TTR has a balance and an instrumented shaft flex-coupling to measure all six components of loads on the rotor. The rotor balance has a capacity of 30,000 lb in thrust, 16,000 lb in shear force and 149,333 ft-lb in combined roll and pitch moments. However, balance is designed for only small, residual torque due to bearing friction from the spinning rotor shaft. The shaft flex-coupling is instrumented for torque measurement and has a capacity of 22,338 ft-lb. The calibration-reference axis system is shown in Fig. 5. Table 1 shows the calibration range for the TTR rotor balance.

**Table 1. Rotor Balance Calibration Ranges**

| Load (applied at the hub) | Bell 609 Calibration Range | Balance Design Range |
|---|---|---|
| Normal Force | 15,184 lb | 30,000 lb |
| In-plane Shear | 8250 lb | 10,000 lb |
| Hub Moment | 7500 ft-lb | 60,000 ft-lb |
| Torque | 22,338 ft-lbs | N/A |

## PHOTOGRAMMETRY SYSTEM DESCRIPTION

Photogrammetry is the science of making 3D location measurements from photographs and images. The photogrammetry system used was based on Geodetic Systems, Inc.'s portable Video-Simultaneous Triangulation and Resection System (V-STARS®) software and hardware. These system components were selected for the ability to obtain highly accurate measurements of large, complicated objects, such as the calibration stand, the TTR and calibration hardware.

The V-STARS system consists of a workstation computer, and two ultra-high-resolution digital cameras, an Autobar, two scale bars, and multiple-coded targets. The system measures the 3-dimensional coordinates of points of interest by intersecting the lines of sight from the cameras to the points using a process called triangulation, which follows the single camera photogrammetry principal as discussed in Refs. 4 - 6.

The V-STARS software supports two camera systems: the V-STARS/S system and the V-STARS/M system. The V-STARS/S is a single camera system and was used to align the calibration hardware and develop the control field (calibration files) for the V-STARS/M system.

The V-STARS/M is a dual-camera system and was used to acquire deflection measurements during balance calibration. One of the most powerful features of the dual-camera system is the ability to measure in unstable environments. This was accomplished by placing a number of targets on the FWD Frame, which serve as reference points for the dual-camera system in unstable mode. The coordinates for these points were established by a one-time single-camera measurement to create the control field for the dual-camera system. The V-STARS/M system uses these points to calculate the position and orientation of the cameras each time a deflection measurement is made. Thus, movement of the cameras and the test rig is accounted for in every picture and has no effect on system accuracy. The unstable mode combined with the synchronized strobes enables the system to make accurate measurements if vibrations are present during calibration loads.

## PHOTOGRAMMETRY METHODOLOGY

The photogrammetry system development was initiated and completed prior to buildup of the calibration frame and installation of the TTR. Development utilized 3D modeling software for the determination of camera and target positions. In addition, all potential camera positions were screened to ensure that they met the 60-degree apex-angle required for the V-STARS/M system as discussed in Ref. 7.

### Approach

3D Computer Aided Design (CAD) models of the TTR, the calibration stand and the loading hardware were created and imported into SketchUp[1], a 3D modeling program. In addition, a camera lens model was created and imported into SketchUp to model the V-STARS cameras' fields of view. The 3D model was used to determine nominal camera locations and the camera lens model identified the visual blockage imposed by the TTR, the calibration stand and the loading hardware. The lens model also identified the placement of targets on the metric hardware where both cameras have a line of sight to all the targets, which is required for the dual-camera system to acquire deflection measurements.

For verification of the nominal camera positions identified in the 3D model, a full system checkout of the V-STARS/M system was completed, which included a full-scale foam model of the metric hardware. The TTR, the calibration stand, the loading hardware, and camera support stand were not available to complete a system checkout. Therefore, a foam model of the metric hardware was built to mirror the setup from the 3D SketchUP model to place and access the cameras on the ground floor. The foam model was used to design the alignment and retro-reflective target deflection hardware, determine retro-reflective target size, and verify the camera stations and apex-angle. Figure 6 shows the full-scale foam model and the V-STARS/M system in the lab. A final checkout was completed using the camera support structure after the TTR was installed on the calibration frame.

### Photogrammetric Setup for Hardware Alignment

To prepare the anchor hardware for photogrammetric measurements, special retro-reflective targets were installed on the FWD Frame and the calibration body. Retro-reflective targets provide the necessary contrast needed to accurately identify targets in photogrammetry images. The target material was 4-mil thick, 3M Scotchlite 7610, high-reflectance adhesive tape. To acquire accurate measurements during the calibration process, a minimum of 20 targets (points) and 4-coded targets were required in each measurement image acquired. To satisfy the V-STARS minimum requirements and overcome the visual constraints imposed by the hardware buildup, a total of 2,800 3/8-inch diameter retro-reflective targets and 120 coded targets were evenly (approximately) installed all around the inner faces of

[1] Trimble Navigation, http://sketchup.com, Sunnyvale, CA

the FWD Frame, the calibration body, the TTR, and the rotor balance.

An Autobar and two carbon-fiber scale bars (3-m long), were used for the alignment measurements to define the preliminary origin and set the volumetric scale. The rotor balance coordinate system served as the global origin for all photogrammetric measurements. The coordinate system was established using four equally and radially spaced pin holes located on the flange (base) of the rotor balance. The flange was the closest feature to the balance origin with known dimensions. Four custom-machined, retro-reflective steel button targets were pressed into the pin holes. The custom targets were machined with an accuracy of +/- 0.0005 in to reduce hardware buildup error. The four targets were used to transpose the origin of all alignment measurements to the coordinates of the balance origin as described in Fig. 7.

**Actuator Alignment**

The actuator linkage attachment points were aligned to the metric hardware so that the loads applied to the calibration body would be nearly parallel to the principal axes of the balance coordinate system. The actuator linkage was removed during alignment measurements so that the attachment points were visible and to allow adjustment of the anchor hardware, which is the structural housing for the actuator attachment hardware.

The complex buildup of the calibration stand, the calibration hardware, the TTR, and the instrumentation cables imposed severe visual constraints. Therefore, special alignment hardware was designed and built to place visible alignment targets in precise, offset positions to locate linkage attachment points. The load application points on the calibration body and the link attachment points on the calibration frame were measured and documented using the photogrammetry technique to determine the load path for each actuator fixed in space.

The alignment hardware consisted of several components: the horizontal cross bar, the target holder, custom button targets, adhesive retro-reflective targets, and two alignment plates. The target holder screws into the plug of each anchor and places a retro-reflective target centroid at the link attachment point, perpendicular to the load path as shown in Fig. 8.

On the metric hardware, a single target could not be installed into the pitch and roll moment attachment links, therefore, two targets were used to interpolate the center of the link. The interpolation was accomplished by installing custom buttons with vertically-flush targets into the link attachment on each side of the moment arm as shown in Fig. 9. Heavy-duty magnets were used in between the button targets to prevent the hardware from falling out. To align axial and side force attachment points, button targets were installed onto the shear blocks as shown in Fig. 9. For the normal force attachment point, a target holder was installed on the thrust adaptor plate to position the target at the location of the attachment point.

Torque loads were applied using chains on a sprocket gear. So the two torque loads were applied at points that were tangent to the sprocket. These tangent points were determined by the center of the sprocket, the diameter of the sprocket and the orientation of the sprocket's plane of rotation. The values were determined using measurements of adhesive 3/8-in diameter retro-reflective targets that were installed on every other tooth and on both sides of the torque sprocket. A custom jig was made to install the adhesive targets to achieve radial symmetry.

Two alignment plates measuring 12 x 12 x 0.25 inches and 6 x 12 x 0.25 inches were installed on the on calibration body. Except for the size difference, the alignment plates were similar in design. Each plate has flush and counter-sunk ¼-inch diameter retro-reflective targets made from MIC 6 aluminum tooling plate. The 12x12 inch alignment plate was installed on the thrust adaptor plate and the 6x12 inch alignment plate was installed on the axial negative force block as shown in Fig. 10. The alignment plates were leveled with an inclinometer before that start of each photogrammetry shoot. The alignment plates provide multiple targets on a flat plane that were used to move the origin within the software for alignment verification when combining multiple shoots into one.

The measurement of all 22 interface points was broken into 3 phases and then stitched together as one data set. Phase 1 included AFN, PMN, TQP and NF attachment points. Phase 2 included SFN, RMP, RMN, SFP and NF attachment points. Phase 3 included TQS, AFP, PMP, and NF attachment points. The NF target, the alignment plates, and the adhesive targets on the sprocket were captured in all three phases to align and stitch the three shoots into one and to reduce the alignment error between the shoots.

Over a two-week period, three iterations of hardware adjustment and photogrammetric measurements were completed to improve the alignment between the anchor and metric hardware attachment points. The initial goal to align the interface points was +/-0.06 in, but due to the constraints imposed by the anchor hardware and FWD Frame and limited time, not all anchors were aligned within the threshold. Most importantly, the XYZ location of the attachment points was measured relative to the balance origin with an accuracy of one sigma. Fig. 11 shows the final triangulation of the measured points. All the targets on the FWD Frame, anchor hardware and calibration body were removed and the interface hardware was installed.

**Photogrammetric setup for Deflection Measurements**

The metric hardware was set up with deflection targets and fill-in targets. The fill-in targets were used to meet the minimum V-STARS software requirements when measuring the control field along with the deflection targets. During deflection measurements, the fill-in targets were purposely covered to avoid potential target identification problems

during deflection measurements because these targets were not visible to both cameras.

The photogrammetric setup to measure the control field for the deflections measurements was more difficult than the setup for alignment measurements, as the interface hardware was installed and the link attachment points on the metric hardware were blocked from view. To deal with this issue, deflection hardware was designed so that retro-reflective targets could be installed to interpolate the link attachments points on the calibration body. This was not feasible for attachment points on the FWD Frame, so they could not be measured during calibration. However, the FWD Frame was designed so that deflections under calibration loads would be insignificant.

The deflection hardware consist of precision-machined components: the extension brackets, the deflection cross, and frames constructed of modular aluminum T-slot framing from 80/20® Inc.[2] The design was driven by the hardware buildup between the interface hardware and metric hardware shown in Fig. 12. The majority of the hardware was designed during the bench calibration of the V-STARS/M system.

A total of eight extension brackets were installed on the metric hardware; two for each moment arm. The extension brackets were a two-piece design comprised of a support frame and an extension. The support frame was bolted to the moment arm with tight-fitting hardware to remove slop. The extension was located at the center of the support frame with a swivel bolt and can support up to five flush targets. The extension brackets were designed to place 3/8-inch diameter retro-reflective targets at equal distance on each side of the moment arm as shown in Fig. 13. The software can then compute an interpolated point at the link attachment point. The extension allows for the retro-reflective targets to rotate in-line with the axis between the two targets as shown in Fig. 14. The target viewing angle for each camera is therefore improved, increasing target reflectivity, which improves centroid accuracy. These extension brackets were used to interpolate the link attachment points for pitch moment and roll moment. In addition, the (8) targets were combined together to interpolate the center of the metric hardware.

The deflection cross was installed on the thrust adaptor plate for measuring deflections due to torque and shear loads on the rotor shaft and torque on the metric hardware. Custom button targets were installed at the end of each cross arm. The deflection cross was designed to allow for radial and forward adjustment of the button targets to avoid blocking the camera view. In addition, the carbon fiber tubes holding the button targets allowed the targets to rotate in order to improve the viewing angle of the targets for each camera. Figure 15 shows the design of the deflection cross.

Half-inch diameter adhesive retro-reflective targets were installed on the aft face of the moment arms. These targets were used to determine the orientation of the metric hardware, and create the control field for the dual-camera system.

The 80/20 hardware was installed on the upper two rotor quadrants and at the base of the FWD Frame as shown in Fig. 16. The 80/20 hardware was bolted and clamped to the I-beams in tension to prevent movement when vibrations were present. Thirty 5-in square steel plates were installed on the 80/20 hardware with one bolt and a locking washer. Coded targets were installed on the steel plates using heavy-duty adhesive magnets. In addition to the coded targets, three ½-in diameter adhesive retro-reflective targets were installed on each plate in order to have 256 reference points for the V-STARS/M system (system requires a minimum of 50 reference points). The X and Y position of the coded targets were manually adjustable to ensure the coded targets were visible by both cameras during deflection measurements. In addition, the 80/20 support frame was installed at an angle to place the coded targets out-of-plane to increase the calibration volume in the Z-direction.

The alignment hardware and deflection hardware was painted matte black. The ground floor and the second floor on the FWD Frame were vacuumed to remove metal shavings to reduce the number of unwanted scans (bad targets) for each measurement taken. Figure 16 shows the installation of the deflection targets.

**Camera Setup**

Two identical cameras were used to acquire deflection measurements during balance calibration. Each camera has a 2K x 2K sensor, a 21-mm lens (fixed focal length) and a flash ring. The cameras were synchronized with the following settings: flash power = 9, shutter speed = 0.1 s, and f-stop = 18.

Two support structures, one for each camera were installed on each side of the TTR. The support structure for each camera included: off-the-shelf 16-ft high aluminum staging truss, a camera boom, a tilt-head, and three steel cables. The support structure placed the cameras nominally 19-ft above the ground. The aluminum staging trusses were selected for their light weight construction, solid conical connectors and tapered pins for quick and secure assembly. The trusses were bolted to the steel floor and three steel cables were tethered from the top of the truss to the floor for added rigidity at the camera locations. The camera boom allowed for coarse camera adjustment and the tilt-head mounted at the end of the

[2] 80/20 Inc., https://8020.net, Columbia City, IN.

boom provided a finer camera adjustment. The combination of the camera boom and the tilt-head provided six degrees of freedom (DOF) of movement. The 6 DOF allowed the cameras to be adjusted to avoid blockage (electronic hardware and cables) that was not modeled in the 3D SketchUp model. Cables tethered the cameras to the top of the boom for safety reasons. The camera support structure is shown in Fig. 17.

The camera support structures were installed 12-ft apart from each other and 12-ft aft of the metric hardware. The spacing between the support structures in combination with the camera boom ensured the optical axes of the cameras intersected at an angle between 60 and 65 degrees, which is the optimum apex-angle for the V-STARS/M system as described in Ref. 7. Figure 18 shows a plan view of the camera locations.

The cables to power and remotely trigger the cameras were routed from the top of the trusses to the control box located on the first floor next to the TTR. The control box provided clean power to the cameras and filtered out electronic noise. An RJ-45 cable was routed from the control box to the control room. The cameras were remotely triggered from the control room with a workstation laptop.

## CAMERA CALIBRATION

### Alignment Measurements

The single camera system required multiple steps to maintain the camera self-calibration in order to acquire accurate measurements.

The first step involves focusing and setting the correct exposure to easily find and measure the targets. The second step requires the camera to be rolled (90-deg) for half of the measurements in order for the camera to self-calibrate. Lastly, the V-STARS software requires coded targets, an Autobar, and two scale bars in order to triangulate the position of the targets and set the scale for the 3D measurements.

The single camera system has a 24-mm wide angle (fixed focal length lens) and was designed to focus on points between 0.5 m (20 in) and 60 m (200 ft) from the camera, effectively eliminating the depth of focus problem. The depth of field permitted placement of retro-reflective targets all around the FWD Frame and calibration body.

Retro-reflective targets were selected to insure that the target and the background exposures were independent of each other. The target exposure is determined by the power of the ring flash, while the background exposure is determined by the ambient lighting, which is controlled by the shutter speed. The goal is to have bright, but not saturated, target images that are easily distinguished from the background. Several test shots with different strobe power and shutter settings were tested to improve the exposure of the retro-reflective targets against the gloss white paint of the FWD Frame, the TTR body and the bare metal hardware. For each test shot, the grayscale values for each target were inspected to verify the target was not over- or under-exposed.

To self-calibrate the camera during alignment measurements, the camera was rolled 90-deg for every other picture taken. Rolling the camera calibrated the camera at the time of measurement, which is far superior to relying on lab calibrations. In addition, multiple camera stations were screened prior to the start of the alignment measurements. Eight to ten pictures were acquired for each camera station.

For improved accuracy, the coded targets, an Autobar, and two scale bars were used during photogrammetry measurements. The coded targets are used to stitch the images together when the data is processed, the Autobar defines the global coordinate system, and the scale bars are used to set the scale for all measurements. The software then determines the final orientation of the camera stations in order to triangulate the measured targets.

To verify the accuracy of the camera settings and photogrammetric setup, the scale bars and the Autobar measured values were compared to the calibration certificates.

### Deflection Measurements

For the dual-camera system, the camera calibration required a four-step process to develop the control field.

The first step involved setting up the V-STARS hardware on the calibration body, which includes: coded targets, an Auto bar, and two scale-bars to meet the V-STARS system requirements.

During the second step, all the points on the calibration body and 80/20 hardware were measured. Images were captured all around the calibration body and processed. To verify the measurements were accurate and to scale, the scale bars and the Autobar measured values were compared to the calibration certificates.

The third step involved culling the data and verifying all the critical points were captured with an accuracy of one sigma or less. The unwanted scans (orphan points) were globally deleted and the image set was reprocessed. After the aforementioned was completed, the coded targets, the Auto bar, and two scale bars were carefully removed from the calibration body. In addition, the fill-in targets were covered.

Lastly, to create the control field for the dual camera system. The Autobar origin was transposed to the balance origin using the four points located at the base of the rotor balance. After the global origin was transposed, the points for the coded targets, the Auto bar, and the two scale bars were removed. The control field was then separated into two sets of points; the detail points and driver points. The detail file only included the points that were installed on the metric hardware.

The driver file included all the points on the 80/20® hardware that were used as the reference points for camera orientation. To verify the accuracy of the control field, 50 static images were taken before and after each calibration run. The sigma values of each measured point were used to verify the accuracy of the control field before, during, and after each calibration run. Figure 19 shows the driver and detail points.

The control field was measured once a week and after each hardware configuration change. In addition, the V-STARS/M system was set to unstable mode and the strobe power and shutter speed for each camera were synchronized to maintain system accuracy throughout the entire calibration process.

## QUALITY ASSURANCE

### Challenges

Acquiring photogrammetric measurements was difficult due to the construction and buildup of the calibration stand and calibration body. A 21-mm viewfinder was used to study the blockage and determine the camera stations for the alignment measurements and to generate the control field. The camera stations were marked on the ground and the vertical positions were dictated by the surrounding hardware.

To verify each camera station, the wireless card on the camera was used to communicate with the computer. The wireless card provided real-time measurements and allowed for quick validation. To validate each camera station, a minimum of 6 coded targets and 20 individual targets were required for each picture taken.

The camera viewfinder was not used for all camera stations. Instead, laser pointers were used in small, tight areas to align the optical axis of the camera to a cluster of targets. Marking the camera stations and using the wireless card with the laser pointers yielded repeatable measurements and consistent accuracy throughout the entire calibration phase. Figure 20 shows the camera stations used for the alignment measurements and for generating the control field.

In the early stages of the deflection measurements, during configuration 1, the region of interest (ROI) of two targets would appear very close to each other under large deflections. As a result, the software would incorrectly swap the labels of the two targets. To mitigate the problem, a dedicated loading sequence, with large deflections, was developed to test possible solutions. As a result, the inner targets for each arm were removed to avoid target mislabeling and the ROI of the outer-most target was increased in order to capture the target at its largest displacement (when applying 5,930 ft-lb of torque to the rotor shaft).

In configuration 2, several points yielded high sigma errors. Upon further investigation, the system was found to register metal shavings and glossy paint highlights as targets that were in close proximity to the retro-reflective targets. These false targets caused the centroid of each true target to shift; resulting in high sigma errors. To mitigate the problem, a black pen was used to cover the highlights on multiple locations of the metric hardware and the FWD Frame. In addition, the floors were vacuumed to remove debris.

## DATA ACQUISITION

Each load condition was applied for 30 seconds. The deflection measurement was manually triggered 10 seconds into each load condition and two image pairs and a triangulation file were acquired for each load point. The sigma values for the measured points were quickly scanned before proceeding to the next load condition. The photogrammetry system acquired 4,002 load measurements during the rotor balance calibration period, which included three base hardware configurations and six extended load configurations for diagnostic checks.

## DATA PROCESSING

The location and direction of forces applied to the balance was based on the estimated positions of the attachment points shown in Fig. 11. These positions were measured statically before and after the calibration without the linkages installed, as described previously. Given the strength and rigidity of the FWD Frame structure, the attachment points on the FWD Frame were assumed to be stationary when calibration loads were applied.

During the calibration, the locations of the attachment points on the TTR metric hardware were estimated using photogrammetric measurements of the targets shown in Fig. 21. The V-STARS software determined the moment arm attachment points by averaging the locations of the targets on the extension brackets mounted on both sides of each attachment points. However, the locations of the other attachment points were determined during further post-processing using data exported from the V-STARS system.

The remaining attachment point locations were estimated using the four targets on the cross mounted to the sprocket hardware (Fig. 15). For each calibration load, these four target locations, along with their zero load locations, were used to determine 3D rotation and translation parameters that describe the change in position and orientation of the sprocket hardware under load. The full set of rotation and translation parameters were applied to reference locations of the axial and side force attachment points on the TTR metric hardware. Since the torque attachment points were tangential to the sprocket, even when the sprocket rotated about the z-axis, the parameter for rotation about the z-axis was set to zero before applying the sprocket rotations and translations to the torque attachment point locations. Lastly, the normal force attachment point was assumed to have the same translations and not rigidly rotate with the sprocket hardware. So only the sprocket translation parameters were applied to the normal force attachment point location.

The possibility exists that the position and orientation of the balance center may also change under load. A method was developed to estimate these changes using additional photogrammetry data that was obtained during the

calibration, but a description of that process is beyond the scope of this paper.

## RESULTS

### Alignment Measurements

The alignment of the actuators should be reduced to enable pure loads, but due to size, weight, and physical access to the anchor hardware, aligning the actuators within +/- 0.06 in proved difficult. Most important, the 3D positions of the attachment points were measured in the balance coordinate system. This enabled deflection measurements of the calibration body used to determine the location and direction of forces applied to the rotor balance.

Table 2 shows the pre-balance calibration alignment measurement results before the start of the balance calibration. Table 3 shows the post-balance calibration alignment measurement results three months later. Table 4 shows the average results between the pre-balance and post-balance calibration alignment measurements. The estimated alignment results in table 4 were used to determine the location and direction of the applied loads and to determine the calibration matrix.

### Deflection Measurements

Deflection measurements of all targets were successfully acquired for all three hardware configurations. Figure 22 shows the deflection sequence for the pitch moment (positive) interpolated point for all load combinations in configuration 1. The data shows more movement than expected, up to half an inch lateral movement, which is too much to ignore in the calibration process.

Ideally, calibration loads would be parallel to principle axes of the balance coordinate system. In such a situation, for example, application of a calibration normal force would not apply any off-axis (side or axial) forces. Figure 23 shows the estimated axial and side forces due to applied normal force for all of the load combinations applied in configuration 2, based on photogrammetry measurements. The blue circles show the off-axis force due solely to the misalignment of the normal force link attachment points, which were measured immediately before and after the calibration test. The off-axis forces are proportional to the applied normal force, which in this configuration ranged for zero to 15,000 lb.

These off-axis forces might have been reduced if more time were expended in aligning the attachment points. However, the off-axis forces due to both alignment error and hardware deflection, shown as green crosses in Fig. 23, are much greater, which indicates that hardware deflection under load has much more influence. These points do not fall along a straight line as the deflection offsets vary depending on which of the other calibration loads are being applied simultaneously with the normal force load.

Since one of the calibration goals was to keep applied force uncertainties to less than 5 lb, deflection measurements were a crucial part of the calibration process. Deflection data was acquired for all hardware configurations, but the deflection measurement results were similar between configuration 1 and 2. Therefore, the balance calibration data for configuration 2 will be used for the first wind tunnel entry. Figures 23-33 show the off-axis forces for all forces applied in configuration 2.

## CONCLUDING REMARKS

This paper presented alignment measurements and selected deflection measurement (off-axis forces) results of the Tiltrotor Test Rig Balance 1.0 calibration. The balance calibration was executed prior to the first wind tunnel test entry with the intention of measuring rotor loads with a calibrated multi-component rotor balance. In addition, the experimental technique to identify the load path to enable deflection measurements was presented, showing a new experimental capability to correct the applied loading to reduce the uncertainty in the balance calibration measurements. Accomplishments and findings are summarized below:

1. Digital photogrammetry was used to enhance NASA's capability to accurately calibrate large internal multi-component rotor balances.
2. The alignments of the link attachment points were successfully measured before and after the calibration, which helped identify the load paths.
3. The deflections of the link attachment points on the calibration body were successfully measured during the calibration.
4. Alignment measurements and deflection measurements were a crucial part of the TTR balance calibration process. Alignment measurements alone would not have been sufficient.
5. Off-axis forces (hardware interactions) were determined from deflection measurements for the three hardware configurations and for each load type.

## ACKNOWLEDGMENTS

The authors wish to thank the TTR calibration crew of the National Full-Scale Aerodynamics Complex for enabling the calibration measurements. Particular thanks are extended to Alex Sheikman, Tom Norman, Alan Wadcock (NASA Ames) and Christopher Hartley (Jacobs Engineer). We also greatly appreciate the contributions of Gina Willink and James Kennon (NASA Ames) for their mechanical design work of the photogrammetry hardware. Last, but not least, Christine Gregg, Belen Veras-Alba, and Hailey Cummings (NASA Ames Interns) for their contributions to the bench calibration of the photogrammetry system, Matthew Miller and Steve Gonzales for their support during the alignment measurements (NASA Ames Interns) and Michelle Dominguez for her support during the deflection measurements (NASA Ames Intern).

## REFERENCES

[1]van Aken, J. M., "Analysis of Calibration Data for the Multi-Component Rotor Balance Installed in the NFAC Large Rotor Test Apparatus," Paper AIAA 2007-146, 46th Aerospace Sciences Meeting and Exhibit, Reno, NV, January 8-11, 2007

[2]van Aken, J. M., Shinoda, P. M., Haddad, Farid, "Development of a Calibration Rig For Large Multi-Component Rotor Balance", 46th International Instrumentation Symposium of the Instrument Society of America, Bellevue, WA, April 30th – May 4th, 2010.

[3]Peterson, L. R., van Aken, J. M., "Dynamic Calibration of the NASA Ames Rotor Test Apparatus Steady/Dynamic Rotor Balance," NASA TM 110393, 1996

[4]Dold, J., Peipe, J., "High Resolution Data Acquisition to Observe Moving Objects," International Archives of Photogrammetry and Remote Sensing, Vol. XXXI, (Part 5B), Vienna, 1996

[5]Mikhail, E. M., Introduction to Modern Photogrammetry, John Wiley & Sons, Inc, New York, 2001.

[6]Wolf, P.R., Elements of Photogrammetry, McGraw-Hill, New York, 1974.

[7]Sandwith, Scott, and Cork, Glen, "V-STARS/M System Accuracy Test Results," Coordinate Measurement System Committee Conference, Dearborn, Michigan, July 31ST – Aug 4th, 2000.

**Author contact:**
Eduardo Solis eduardo.solis@nasa.gov
Larry Meyn larry.meyn@nasa.gov

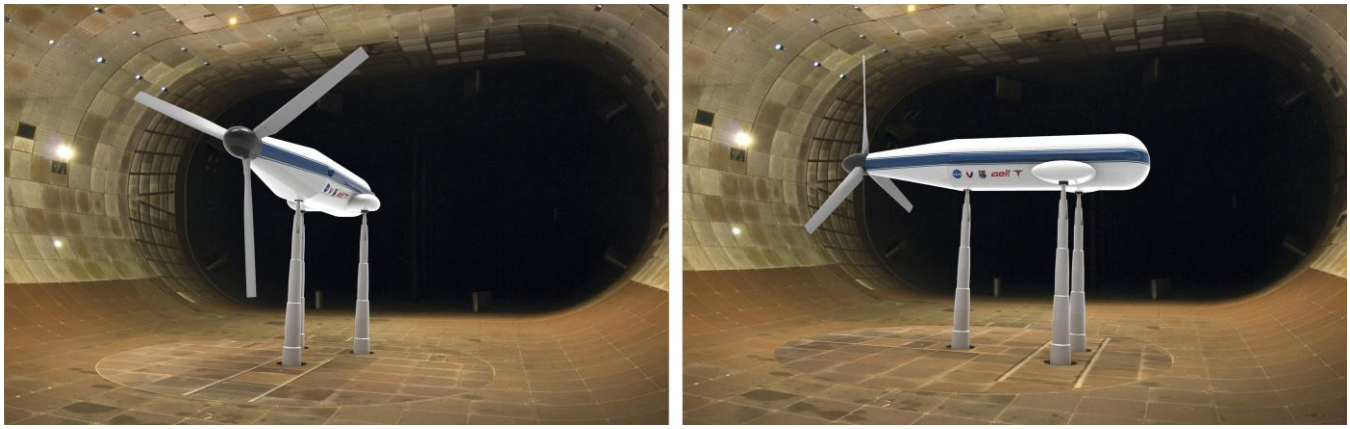

**Figure 1. Renders of the TTR installed in the 40-by 80-Foot Wind Tunnel. (Left) Axial configuration. (Right) Edgewise configuration.**

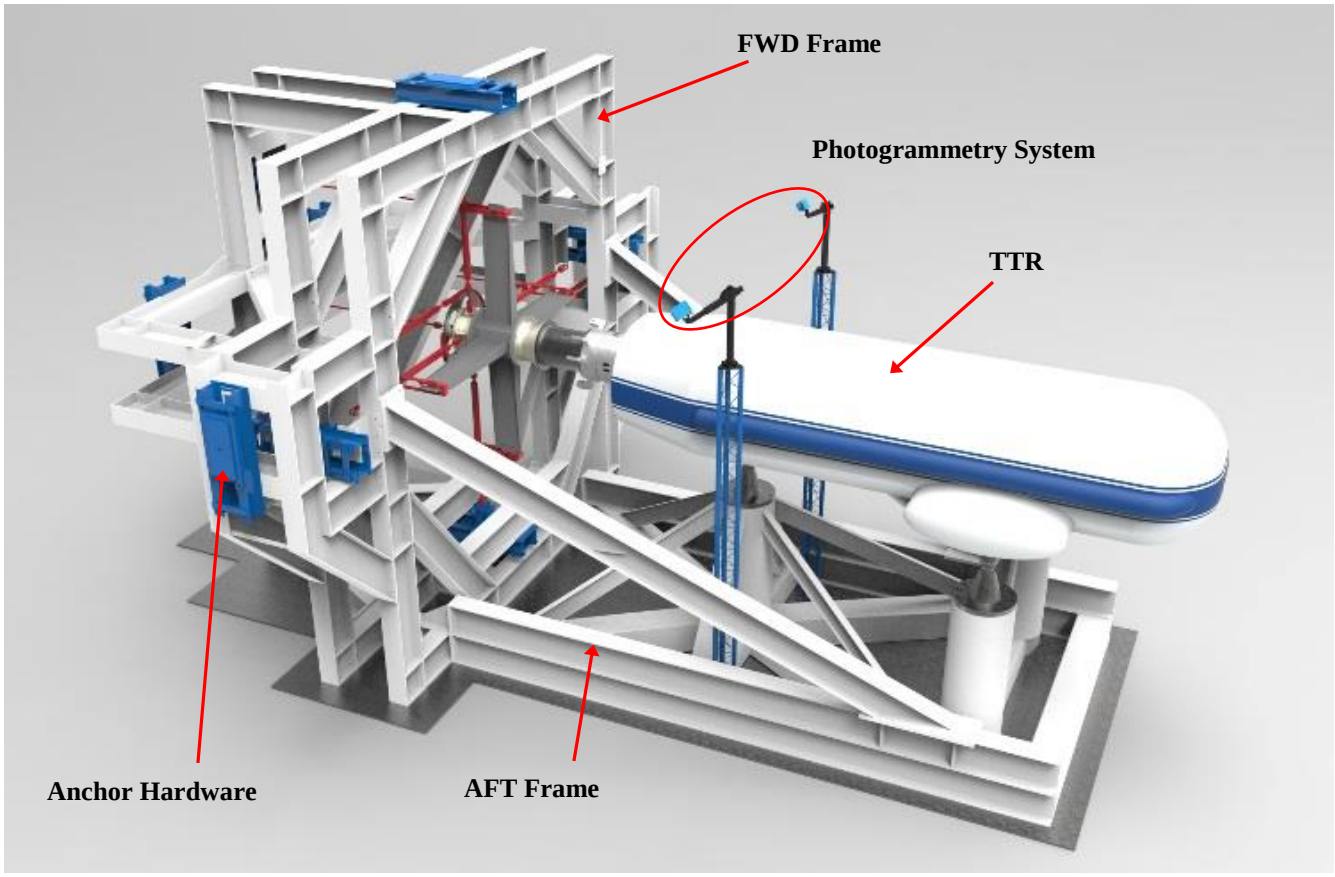


**Figure 2. TTR installed on the calibration stand. The floors on the FWD Frame are removed to better represent the design of the calibration stand.**

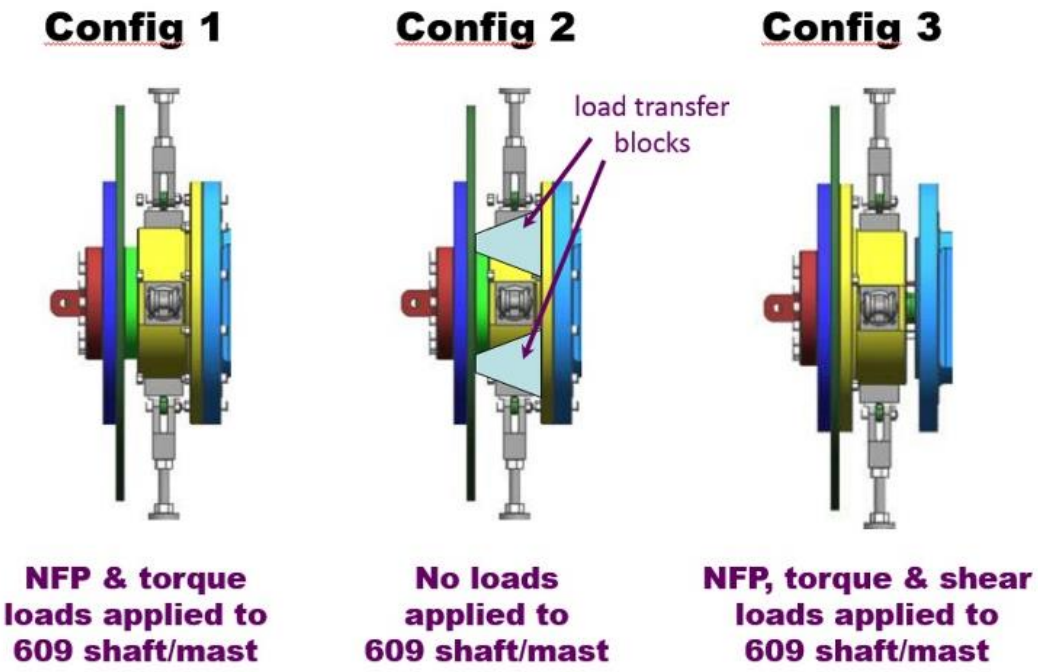


**Figure 3. The forward hardware highlighted in red, dark blue, green, and yellow allowed for three loading configurations for the balance calibration process. Metric hardware is shown in light blue.**

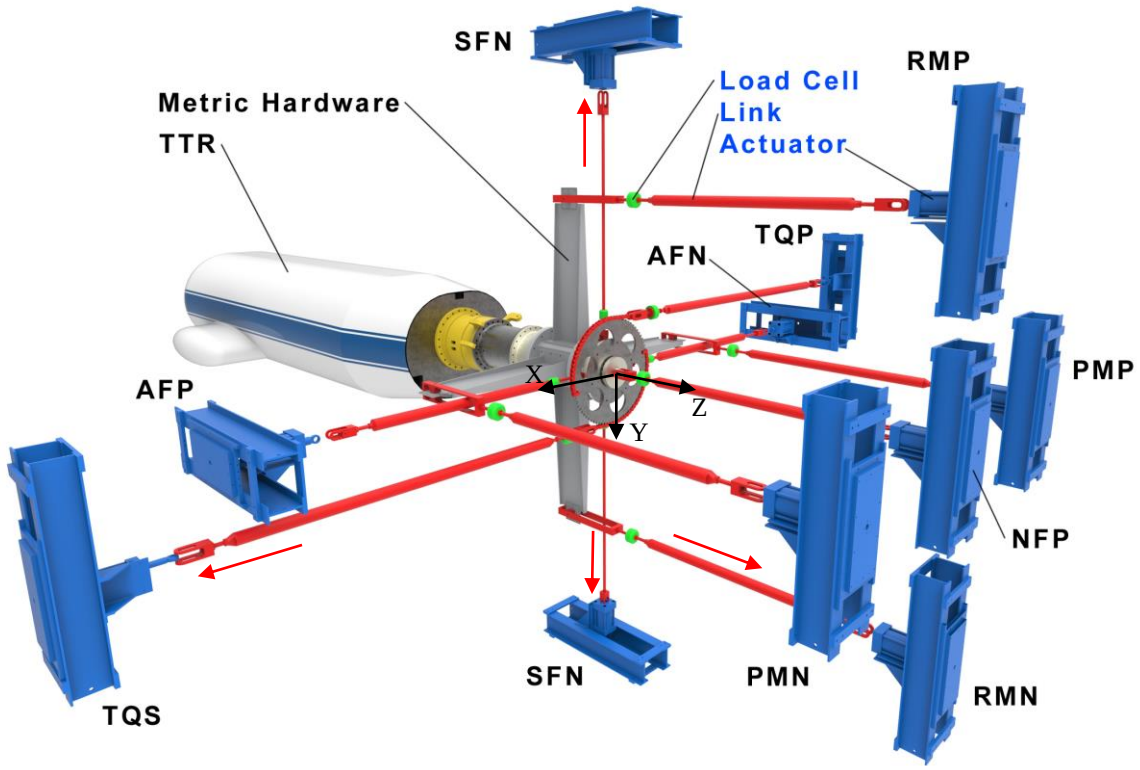


**Figure 4. Calibration hardware loading tree with the FWD Frame and AFT Frame removed. Red arrows represent the load direction.**

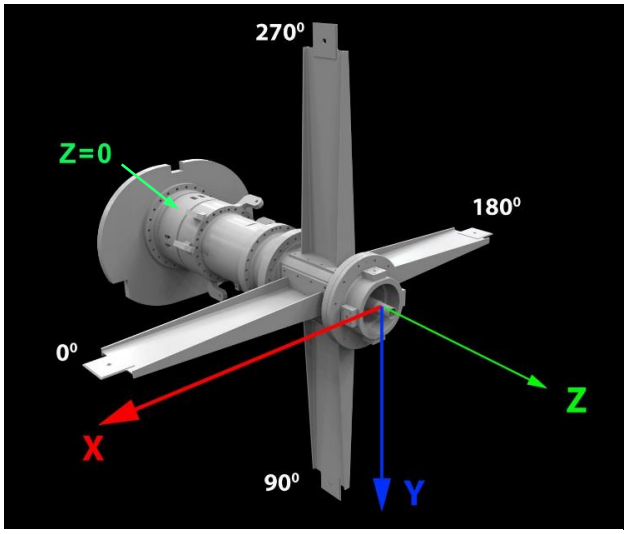


**Figure 5. Balance calibration coordinate system. Balance origin z-axis = 0.**

**Figure 6. Bench calibration of the V-STARS/M system.**

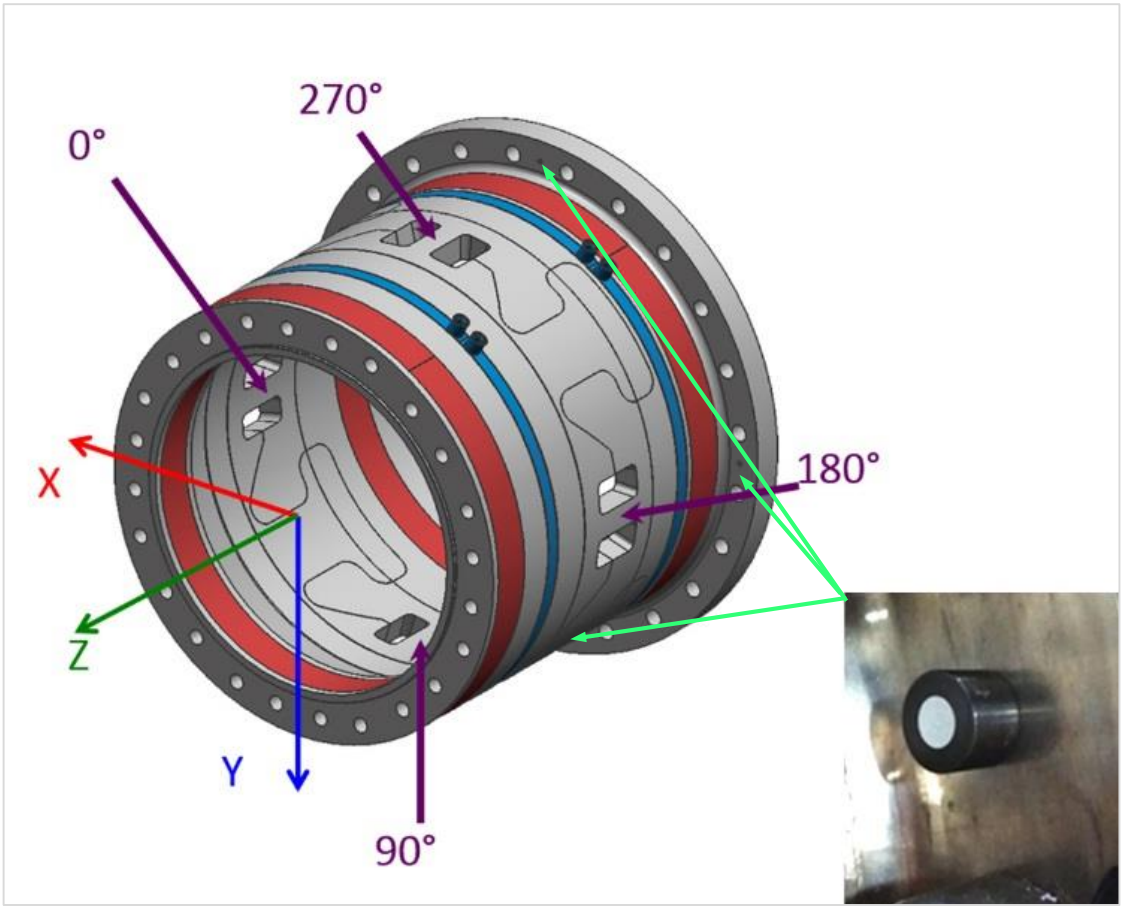


**Figure 7. Four retro-reflective button targets installed on the flange of the rotor balance.**

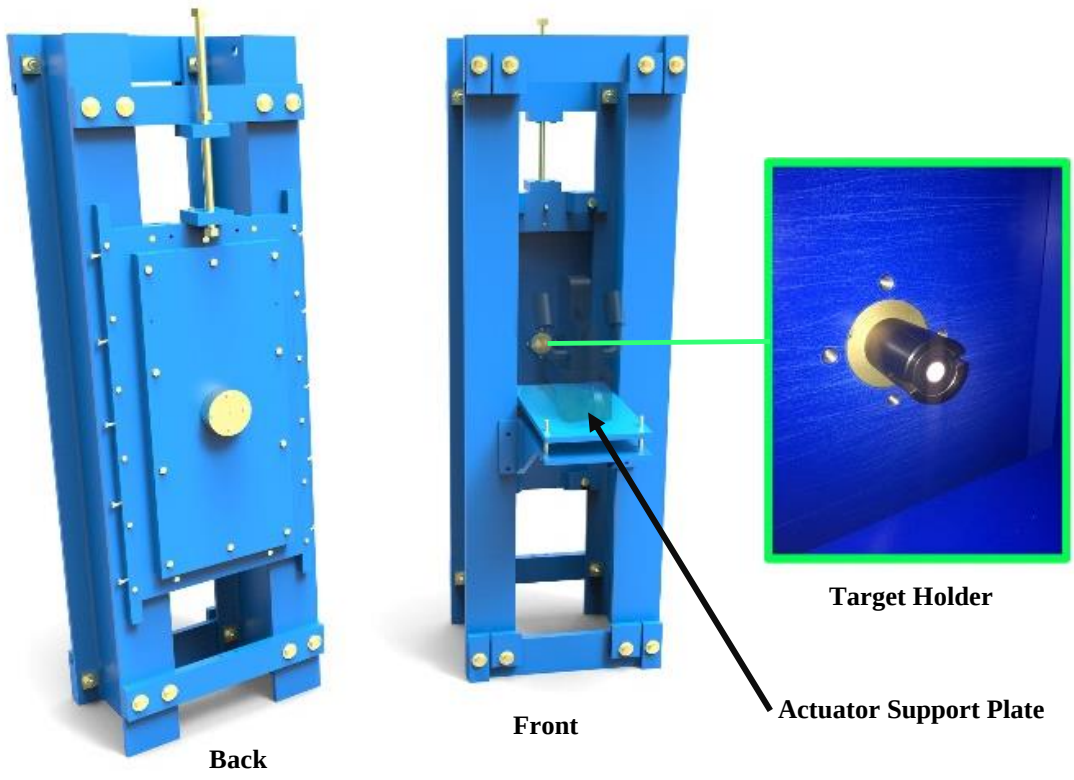


**Figure 8. Anchor hardware design and target holder installation.**

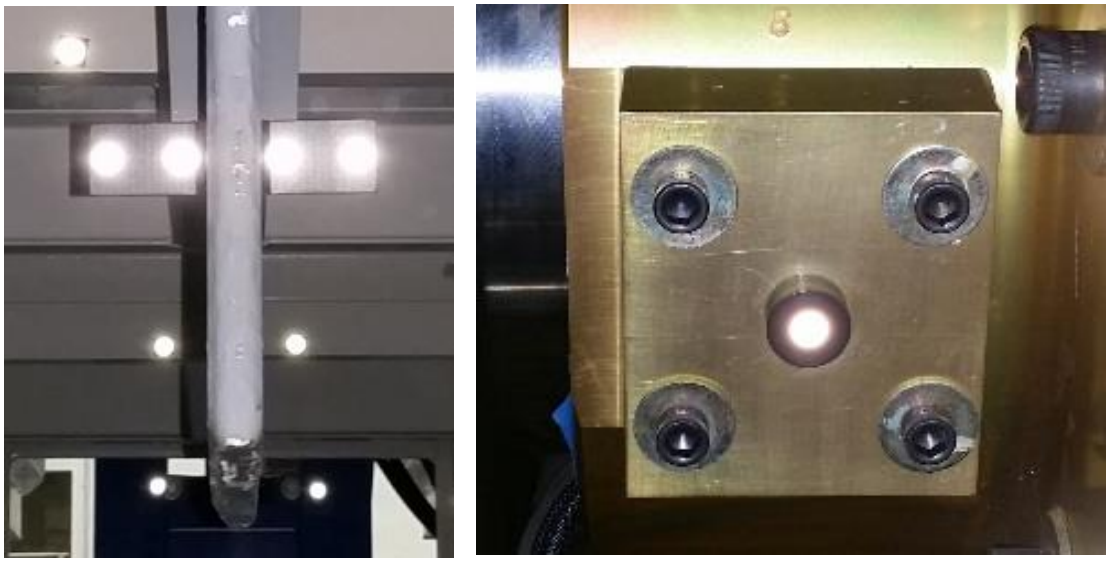

**Figure 9. (Left) Roll moment link with custom button targets installed on each side of the moment arm. (Right) Shear block with retro-reflective button target.**

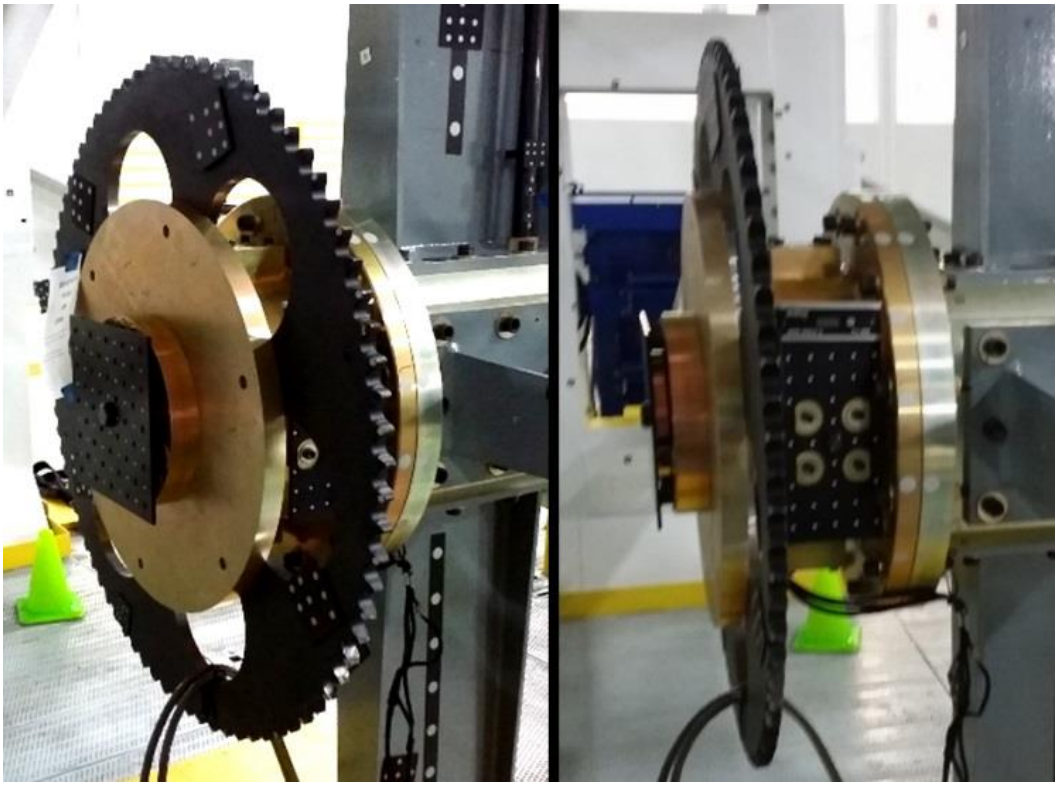

**Figure 10. (Left) 12x12 inch plate installed on the thrust adaptor plate. (Right) 6x12 inch alignment plate installed on the axial negative shear block.**

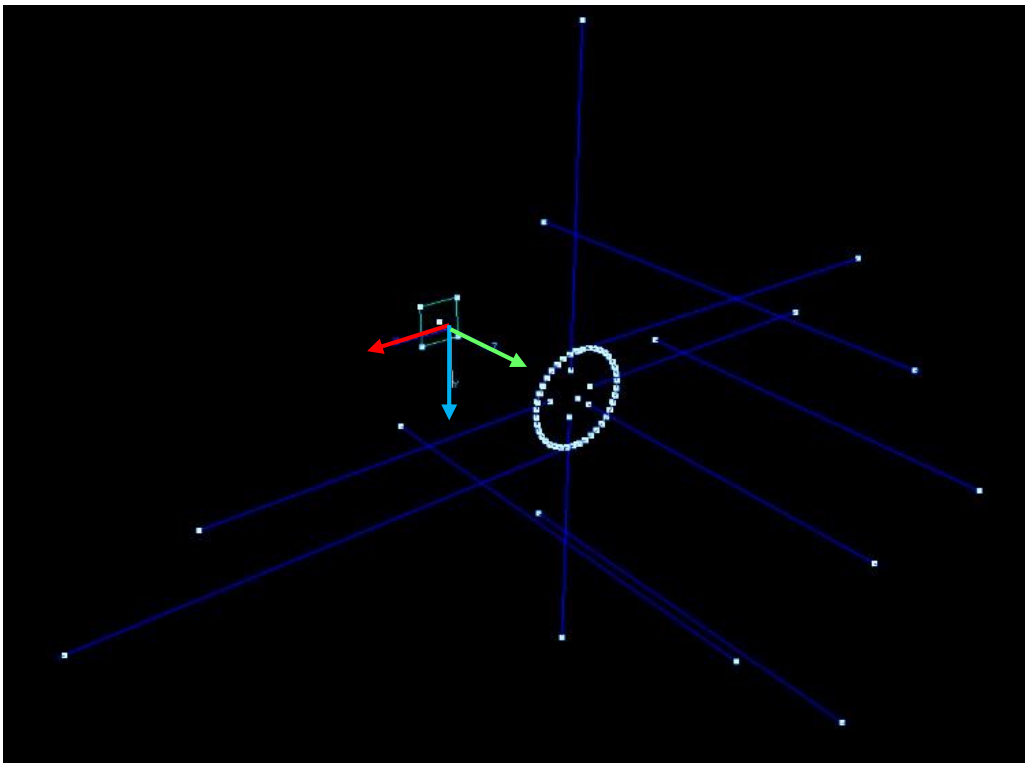

**Figure 11. 3D measurement of the link attachment points. Blue lines represent the load path between the link attachment points.**

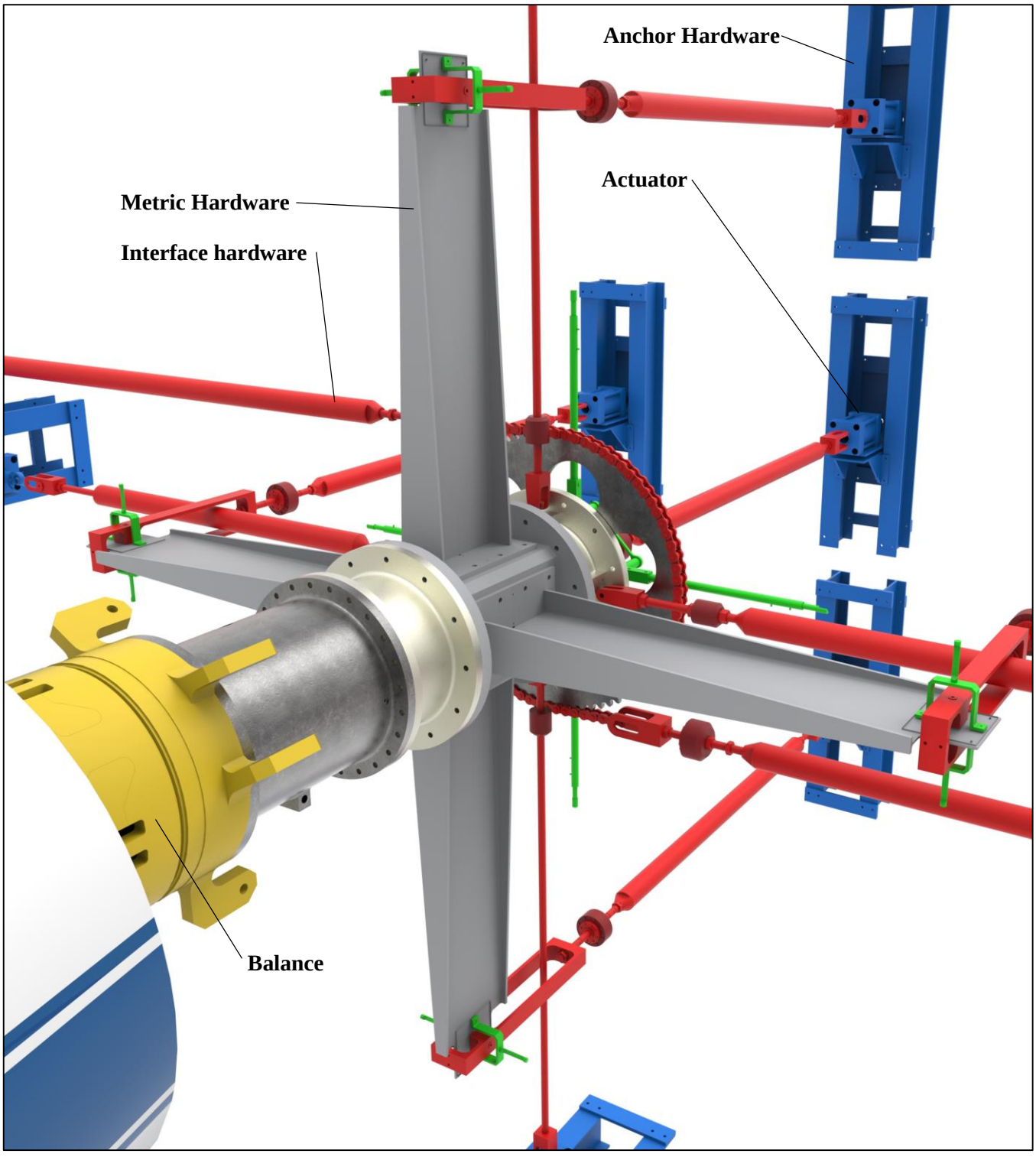


**Figure 12. Interface hardware (red) attached to the moment arms on the metric hardware. Deflection hardware (green) installed around the interface hardware buildup.**

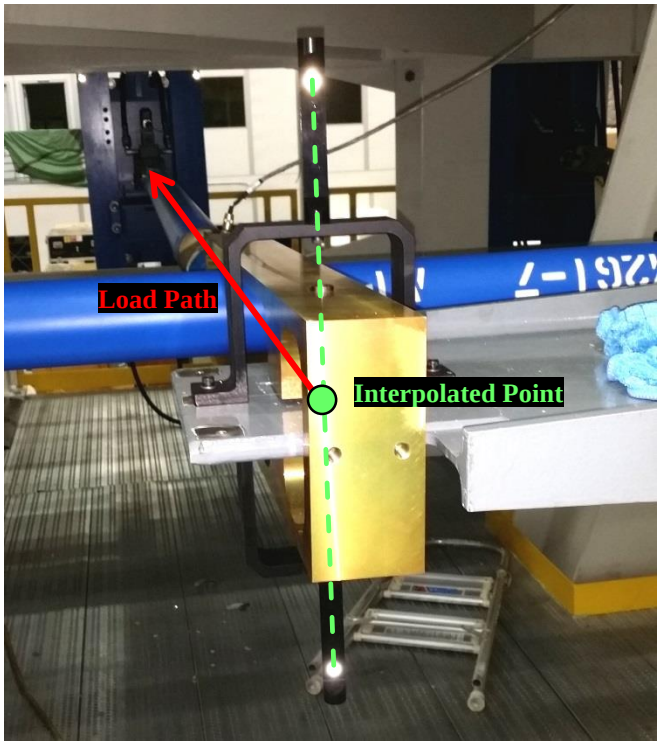


Figure 13. Extension bracket installed on each side of the moment arm.

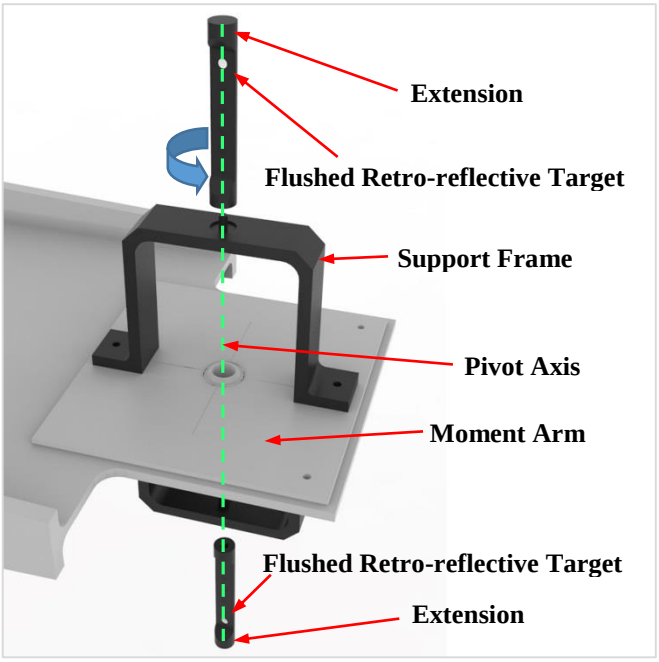


Figure 14. Exploded view of the extension bracket.

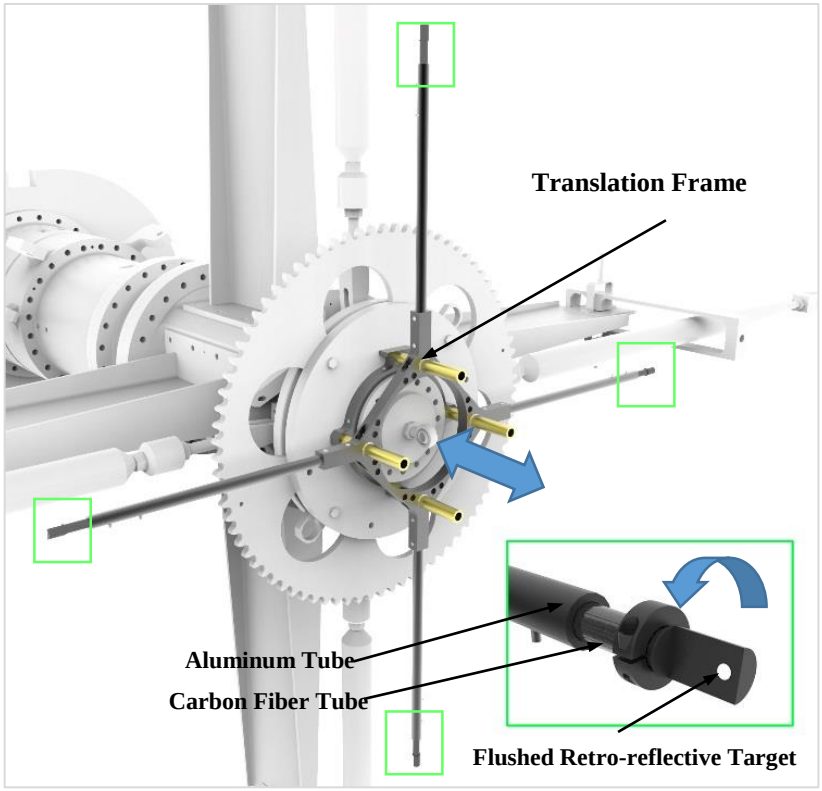


Figure 15. Deflection cross installed on the trust adapter plate. Retro-reflective button targets installed on all four arms.

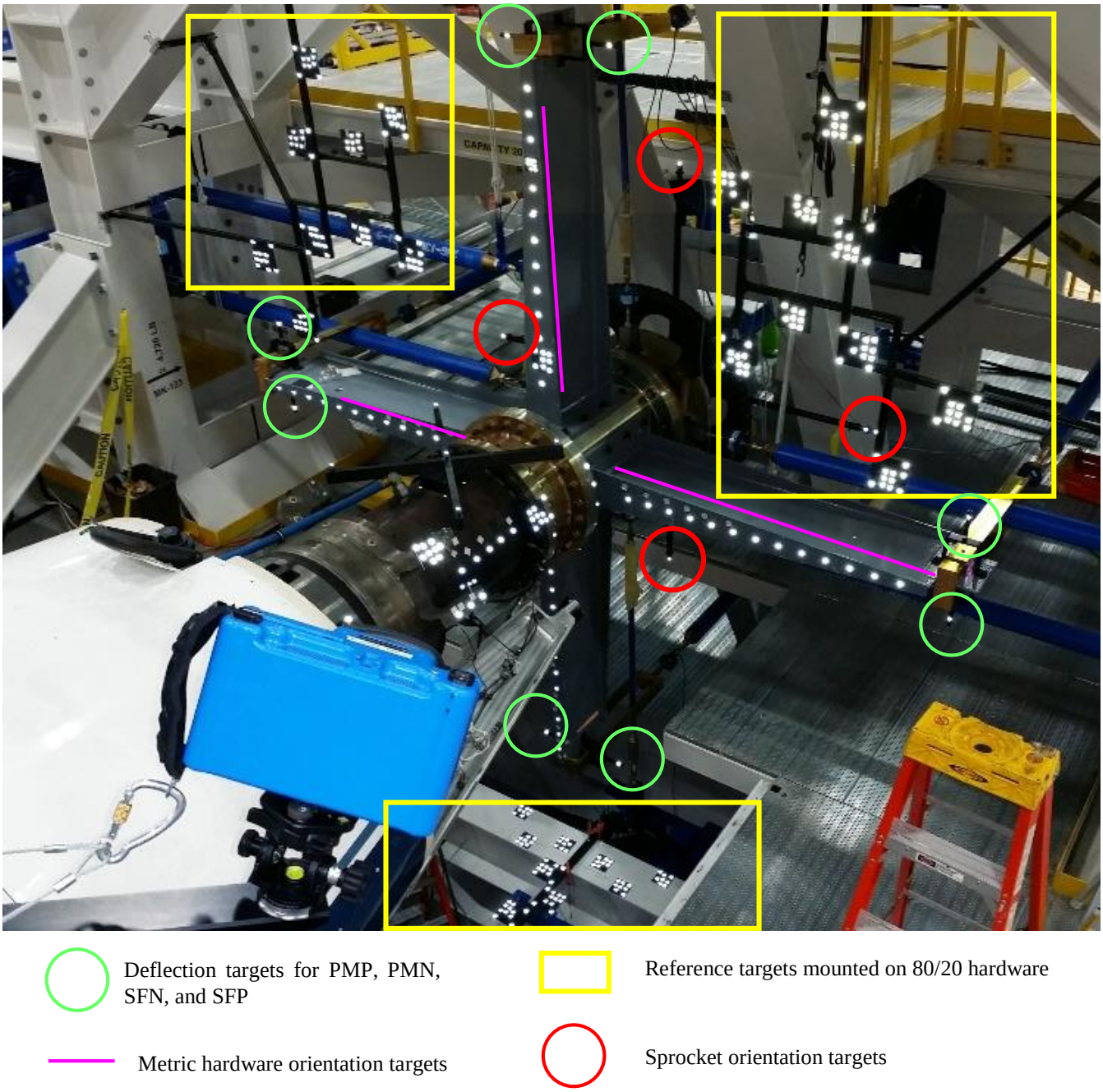


**Figure 16. Deflection hardware installed on the FWD Frame and calibration body, which enabled retro-reflective target installation on the metric hardware.**

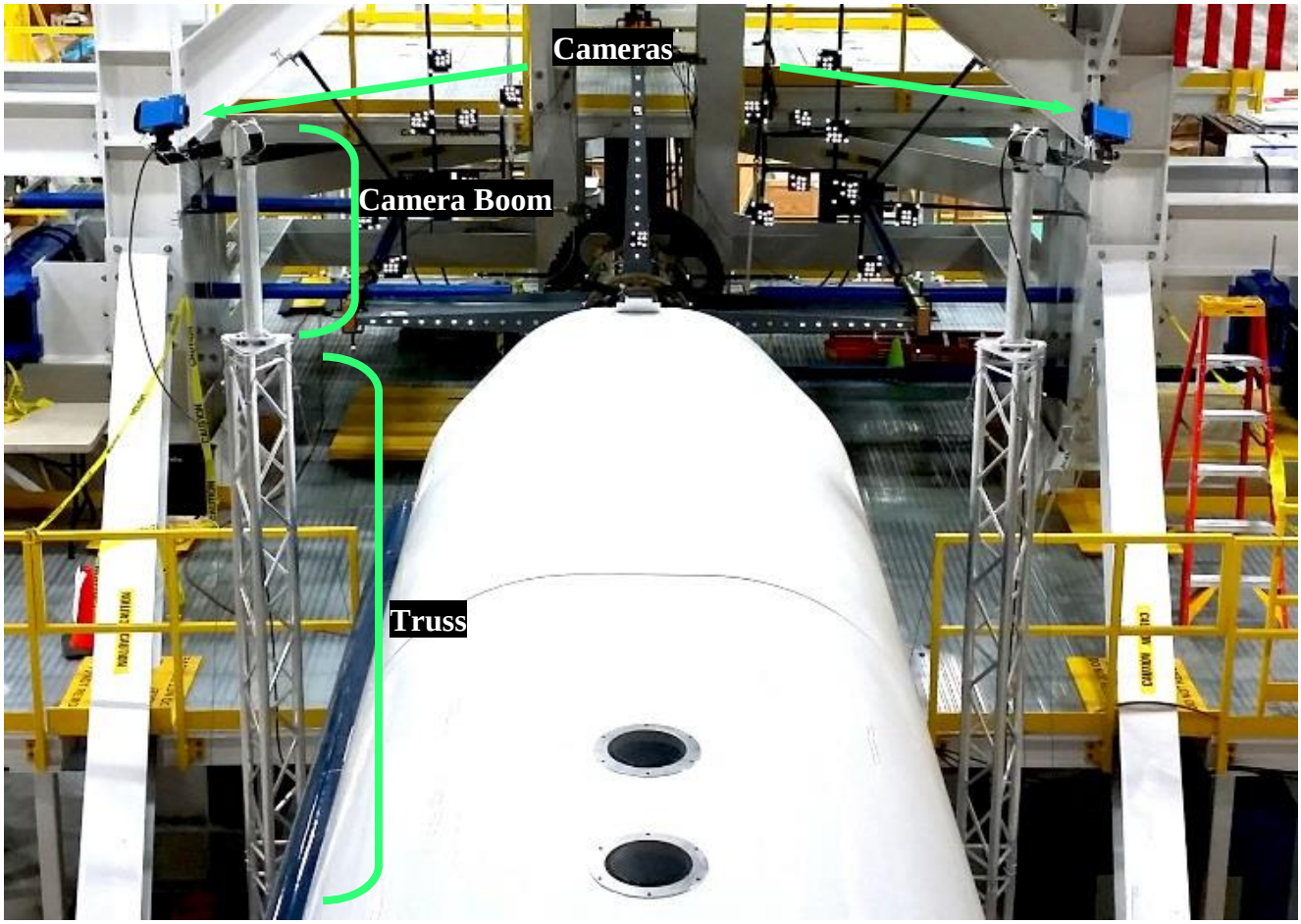


**Figure 17. V-STARS/M system installed on the camera support structures.**

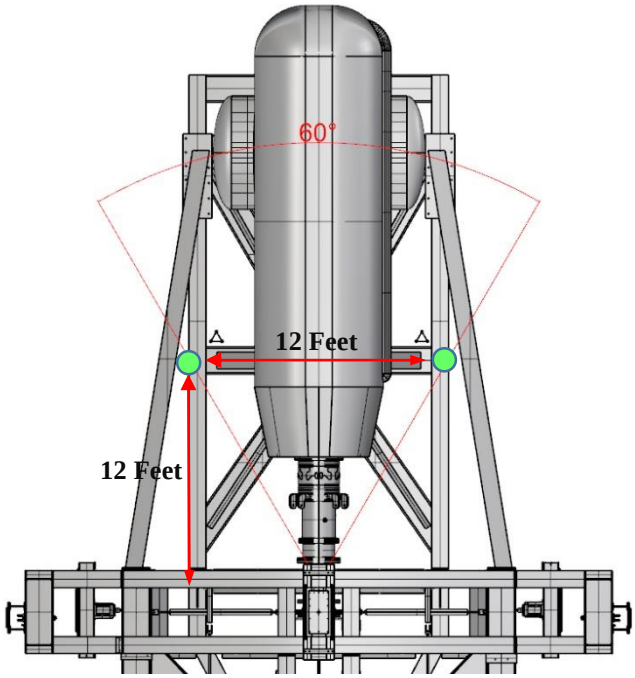


**Figure 18. Plan view of the camera setup. Green dots represent the camera locations. 60 degree apex-angle.**

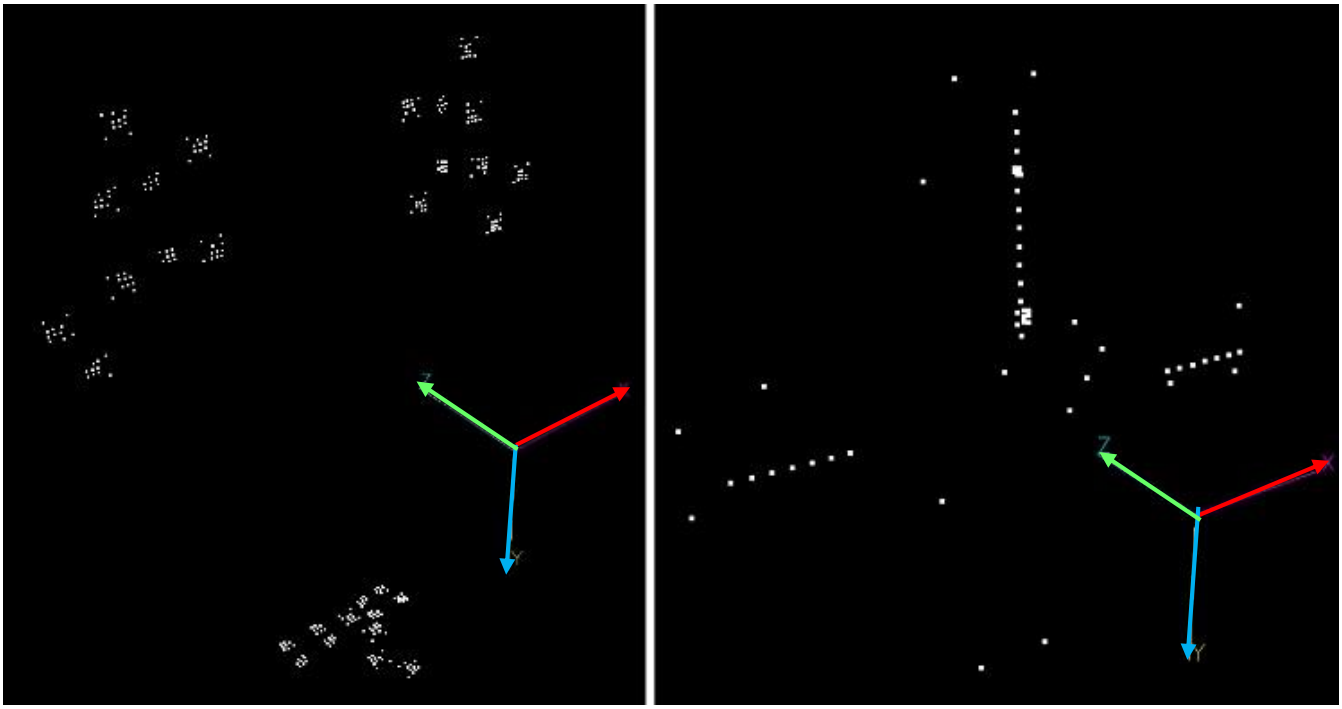

**Figure 19. (Left) Driver (reference) points located on the FWD Frame. (Right) Detail (deflection) points located on the metric hardware.**

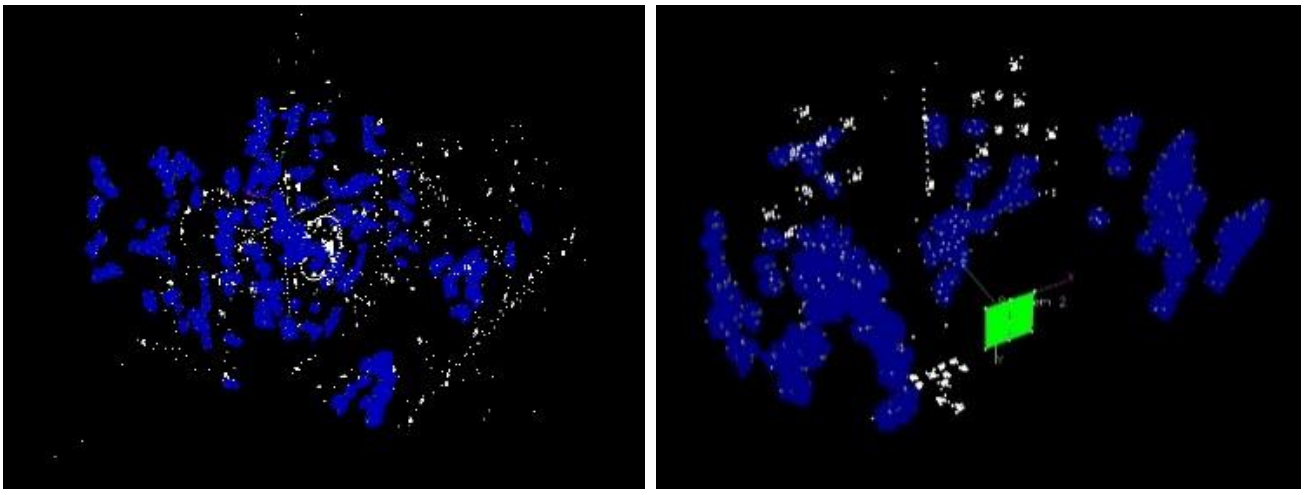

**Figure 20. (Left) Camera stations used for the alignment measurements. (Right) Camera stations used to generate the control field for the dual-camera system.**

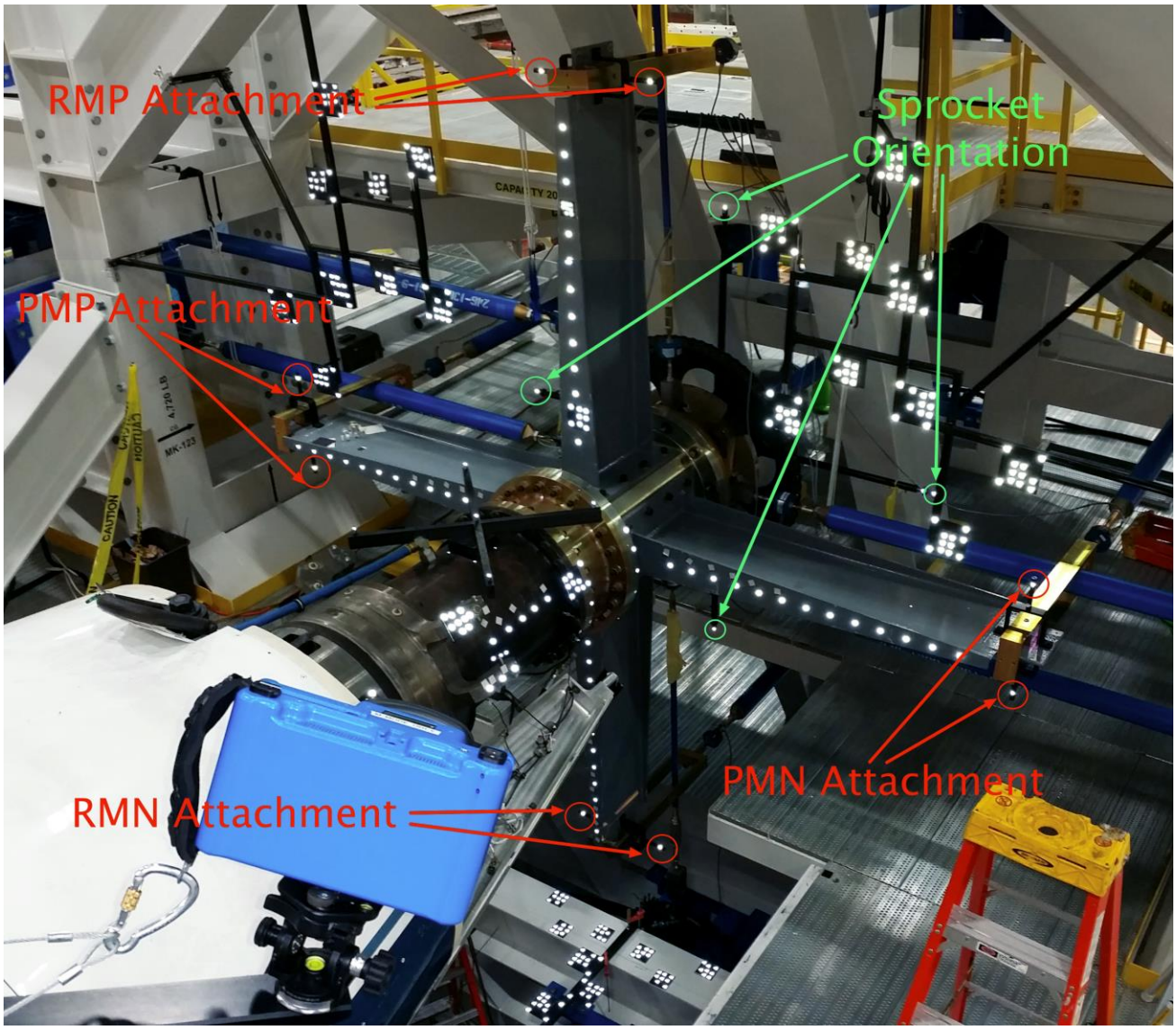


**Figure 21. Deflection targets used to interpolate the link attachment point locations.**

**Table 2. Pre-Balance Calibration Alignment Measurement Results**

| | Forward Frame Attachment Points | | | Metric Hardware Attachment Points | | | Off-Axis Dimensions | | |
|---|---|---|---|---|---|---|---|---|---|
| Actuator | X (in) | Y (in) | Z (in) | X (in) | Y (in) | Z (in) | X (in) | Y (in) | Z (in) |
| AFN | -157.3602 | -0.2808 | 87.8699 | -11.1297 | 0.0284 | 87.7536 | | -0.3092 | 0.1163 |
| AFP | 156.7434 | 0.3734 | 87.8736 | 11.1438 | 0.0347 | 87.7534 | | 0.3387 | 0.1202 |
| NFP | 0.1814 | 0.5182 | 241.3603 | 0.0179 | 0.1143 | 99.7330 | 0.1635 | 0.4039 | |
| PMN | 70.7773 | 0.5607 | 241.5008 | 70.5028 | 0.0766 | 68.4881 | 0.2745 | 0.4841 | |
| PMP | -70.2715 | 0.5009 | 241.4342 | -70.4971 | -0.0127 | 68.5067 | 0.2256 | 0.5136 | |
| RMN | 0.0316 | 71.0290 | 241.2030 | -0.0311 | 70.5266 | 68.4788 | 0.0627 | 0.5024 | |
| RMP | 0.1237 | -69.9057 | 241.4170 | 0.0375 | -70.4707 | 68.5265 | 0.0862 | 0.5650 | |
| SFN | 0.1706 | -149.6414 | 87.7872 | 0.0094 | -11.1077 | 87.7584 | 0.1612 | | 0.0288 |
| SFP | -0.1263 | 131.9423 | 87.7221 | 0.0043 | 11.1625 | 87.7493 | -0.1306 | | -0.0272 |
| TQP | -202.1194 | -22.5932 | 92.9346 | 0.0055 | -22.2072 | 92.6242 | | -0.3860 | 0.3104 |
| TQS | 201.6462 | 22.8529 | 92.3419 | 0.0055 | 22.3728 | 92.6242 | | 0.4801 | -0.2823 |

**Table 3. Post-Balance Calibration Alignment Measurement Results**

| | Forward Frame Attachment Points | | | Metric Hardware Attachment Points | | | Off-Axis Dimensions | | |
|---|---|---|---|---|---|---|---|---|---|
| Actuator | X (in) | Y (in) | Z (in) | X (in) | Y (in) | Z (in) | X (in) | Y (in) | Z (in) |
| AFN | -157.3932 | -0.3134 | 87.8035 | -11.1321 | 0.0020 | 87.7661 | | -0.3154 | 0.0374 |
| AFP | 156.6597 | 0.3610 | 87.8694 | 11.1515 | 0.0021 | 87.7694 | | 0.3589 | 0.1000 |
| NFP | 0.1236 | 0.4442 | 241.4319 | -0.0061 | 0.0738 | 100.0074 | 0.1297 | 0.3704 | |
| PMN | 70.6829 | 0.4816 | 241.4601 | 70.5040 | 0.0577 | 68.5103 | 0.1789 | 0.4239 | |
| PMP | -70.3918 | 0.4253 | 241.3307 | -70.5024 | -0.0385 | 68.5194 | 0.1106 | 0.4638 | |
| RMN | -0.0630 | 70.9286 | 241.4075 | -0.0478 | 70.5110 | 68.5089 | -0.0152 | 0.4176 | |
| RMP | 0.0367 | -69.9889 | 241.4828 | 0.0433 | -70.4962 | 68.5234 | -0.0066 | 0.5073 | |
| SFN | 0.1171 | -149.6585 | 87.7107 | 0.0015 | -11.1304 | 87.7648 | 0.1156 | | -0.0541 |
| SFP | -0.1862 | 131.8827 | 87.7322 | 0.0010 | 11.1441 | 87.7609 | -0.1872 | | -0.0287 |
| TQP | -202.2721 | -22.6168 | 92.8580 | -0.0007 | -22.2379 | 92.6589 | | -0.3789 | 0.1991 |
| TQS | 201.7128 | 22.8316 | 92.3571 | -0.0007 | 22.3371 | 92.6589 | | 0.4945 | -0.3018 |

**Table 4. Average of the Pre-Balance and Post-Balance Calibration Alignment Measurement Results.**

| | Forward Frame Attachment Points | | | Metric Hardware Attachment Points | | | Off-Axis Dimensions | | |
|---|---|---|---|---|---|---|---|---|---|
| Actuator | X (in) | Y (in) | Z (in) | X (in) | Y (in) | Z (in) | X (in) | Y (in) | Z (in) |
| AFN | -157.3767 | -0.2971 | 87.8367 | -11.1309 | 0.0152 | 87.7599 | | -0.3123 | 0.0769 |
| AFP | 156.7016 | 0.3672 | 87.8715 | 11.1477 | 0.0184 | 87.7614 | | 0.3488 | 0.1101 |
| NFP | 0.1525 | 0.4812 | 241.3961 | 0.0059 | 0.0941 | 99.8702 | 0.1466 | 0.3872 | |
| PMN | 70.7301 | 0.5212 | 241.4805 | 70.5034 | 0.0672 | 68.4992 | 0.2267 | 0.4540 | |
| PMP | -70.3317 | 0.4631 | 241.3825 | -70.4998 | -0.0256 | 68.5131 | 0.1681 | 0.4887 | |
| RMN | -0.0157 | 70.9788 | 241.3053 | -0.0395 | 70.5188 | 68.4939 | 0.0238 | 0.4600 | |
| RMP | 0.0802 | -69.9473 | 241.4499 | 0.0404 | -70.4835 | 68.5250 | 0.0398 | 0.5362 | |
| SFN | 0.1439 | -149.6500 | 87.7490 | 0.0055 | -11.1191 | 87.7616 | 0.1384 | | -0.0126 |
| SFP | -0.1563 | 131.9125 | 87.7272 | 0.0027 | 11.1533 | 87.7551 | -0.1589 | | -0.0280 |
| TQP | -202.1958 | -22.6050 | 92.8963 | 0.0024 | -22.2226 | 92.6416 | | -0.3825 | 0.2548 |
| TQS | 201.6795 | 22.8423 | 92.3495 | 0.0024 | 22.3550 | 92.6416 | | 0.4873 | -0.2920 |

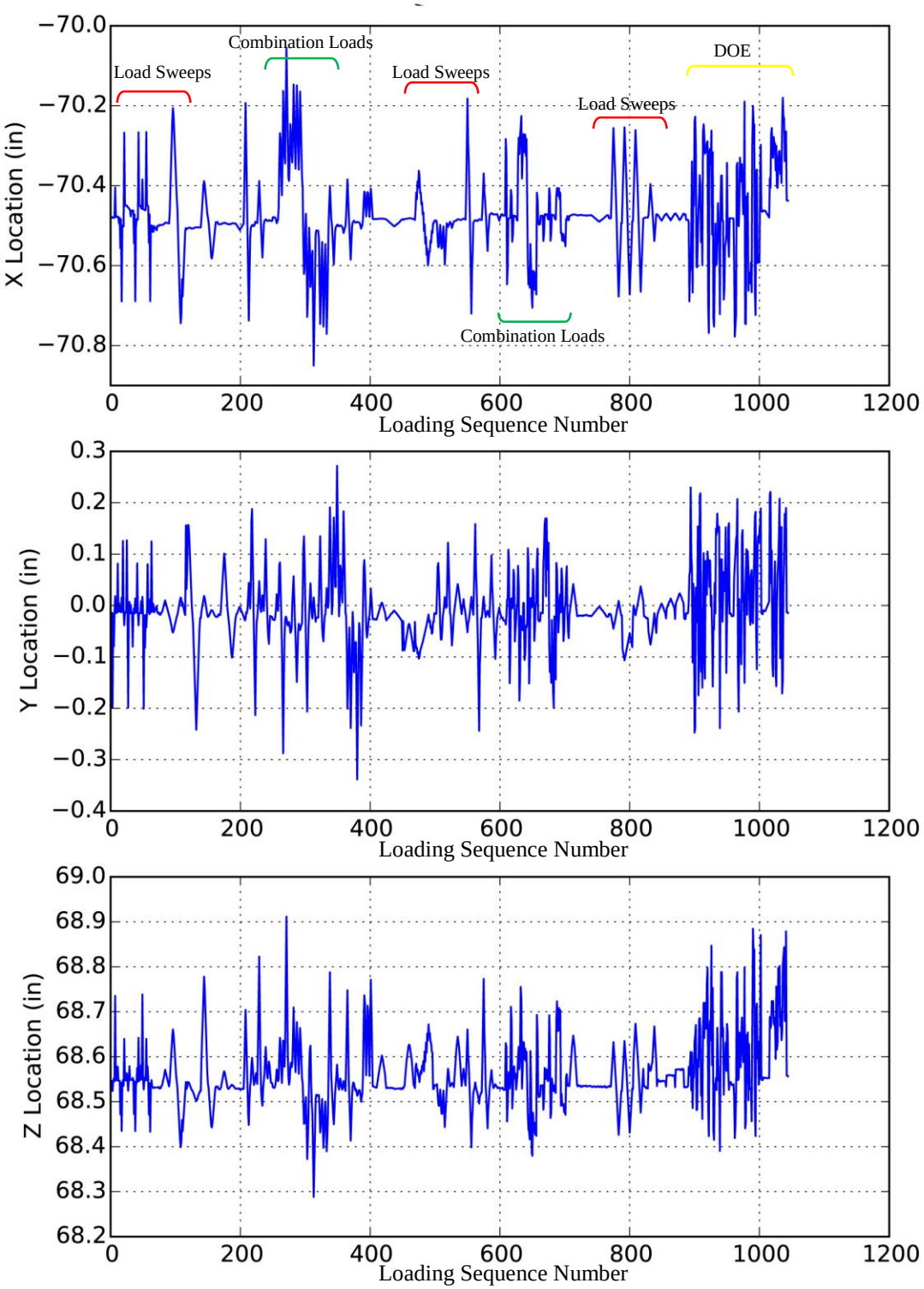


**Figure 22. Deflection history for pitch moment positive interpolated point for all combination loads applied in configuration 1. Up to half an inch in lateral movement. Load application is in the Z-axis.**

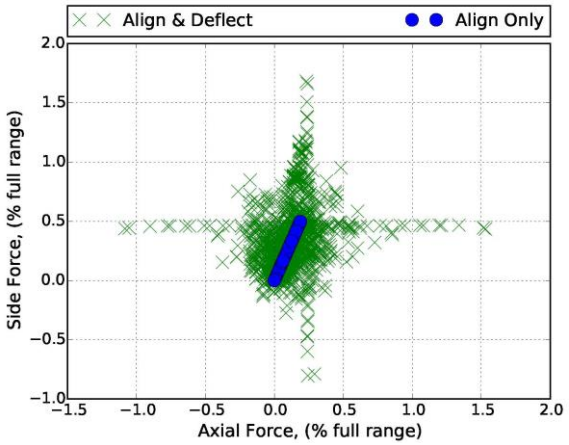


**Figure 23. Side and axial forces due to misalignment of applied normal force for all load combinations in configuration 2.**

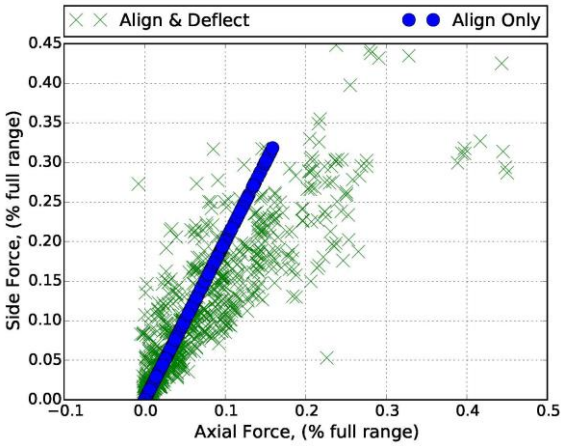


**Figure 26. Side and axial forces due to misalignment of applied pitch moment negative force for all load combinations in configuration 2.**

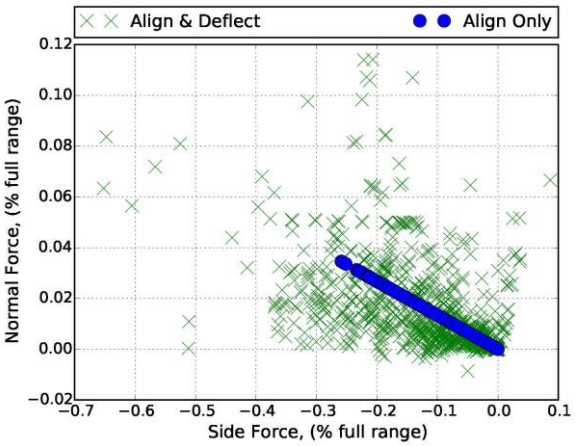


**Figure 24. Normal and side forces due to misalignment of applied axial force negative for all load combinations in configuration 2.**

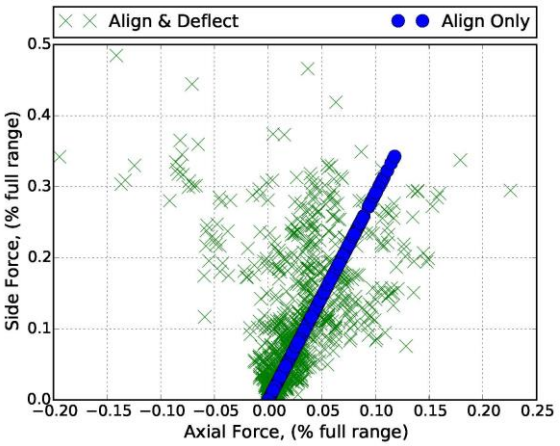


**Figure 27. Side and axial forces due to misalignment of applied pitch moment positive force for all load combinations in configuration 2.**

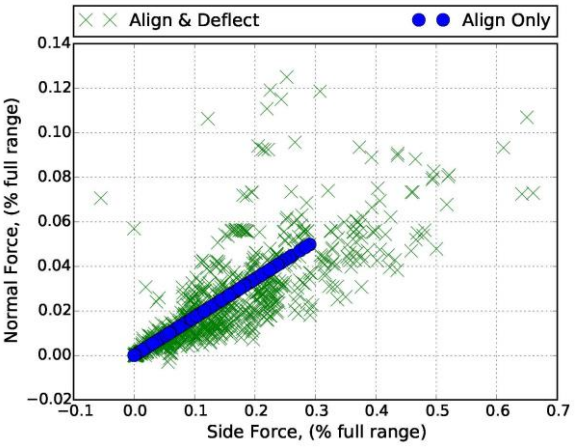


**Figure 25. Normal and side forces due to misalignment of applied axial force positive for all load combinations in configuration 2.**

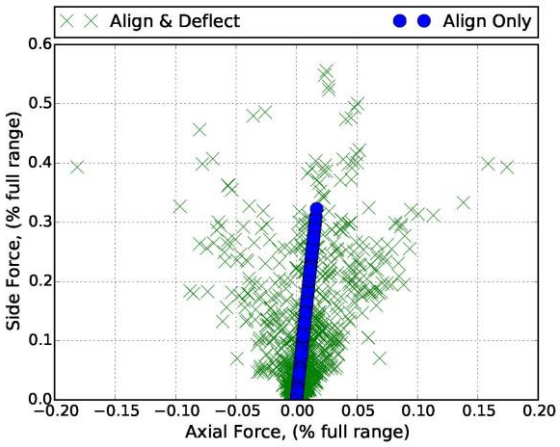


**Figure 28. Side and axial forces due to misalignment of applied roll moment negative force for all load combinations in configuration 2.**

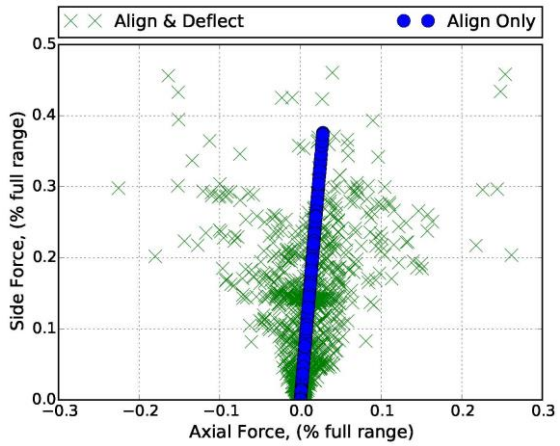


**Figure 29. Side and axial forces due to misalignment of applied roll moment positive force for all load combinations in configuration 2.**

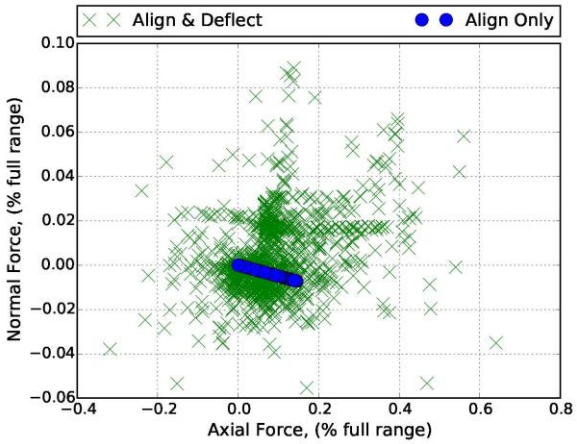


**Figure 30. Normal and axial forces due to misalignment of applied side force negative for all load combinations in configuration 2.**

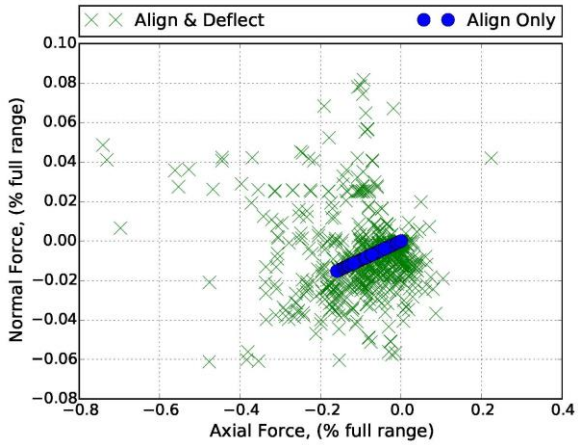


**Figure 31. Normal and axial forces due to misalignment of applied side force positive for all load combinations in configuration 2.**

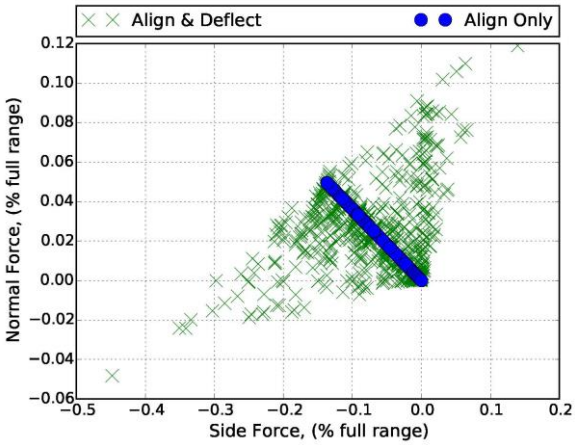


**Figure 32. Normal and side forces due to misalignment of applied torque left force for all load combinations in configuration 2.**

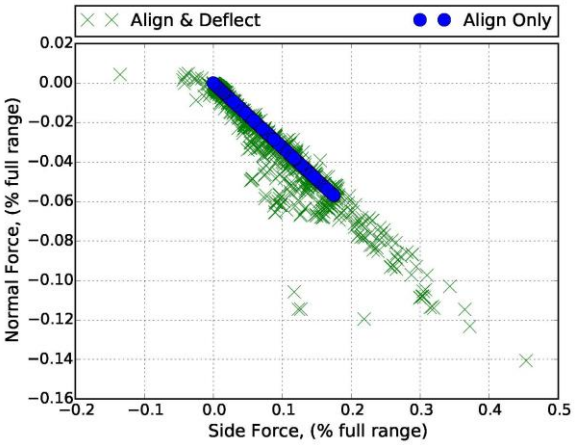


**Figure 33. Normal and side forces due to misalignment of applied torque right force for all load combinations in configuration 2.**